Neutron reflectivity studies of adsorption and wetting in the vicinity of a liquid/liquid critical point: alkane + perfluoroalkane mixtures at a silicon interface

1998 J. Phys.: Condens. Matter 10 8173

(http://iopscience.iop.org/0953-8984/10/37/006)

J. Phys.: Condens. Matter **10** (1998) 8173–8188. Printed in the UK PII: S0953-8984(98)93159-9

Neutron reflectivity studies of adsorption and wetting in the vicinity of a liquid/liquid critical point: alkane + perfluoroalkane mixtures at a silicon interface

James Bowers†‖, Emilio Manzanares-Papayanopoulos‡, Ian A McLure‡ and Robert Cubitt§

† Iwan-N-Stranski Institut für Physikalische und Theoretische Chemie, Technische Universität Berlin, Straße des 17 Juni 112, D-10623, Germany

‡ Department of Chemistry, The University, Sheffield S3 7HF, UK

§ Institut Laue–Langevin, 38042 Grenoble Cédex, France

Received 6 April 1998, in final form 29 June 1998

Abstract. We report the results of a preliminary investigation by specular neutron reflectivity of adsorption and wetting of alkane + perfluoroalkane binary liquid mixtures in the vicinity of the liquid/liquid critical point against a chemically modified (alkane-like) silicon wall. The results suggest the existence of a surprisingly long-ranged profile (≃200–300 Å), even some degrees Kelvin above the upper critical point, and enable us to detect a wetting layer and its liquid/liquid interface below the critical point. The technique is capable of determining the composition, uniformity, and thickness of the wetting layer.

1. Introduction

In the last 20 years the study of wetting phenomena, among them the specific cases of critical adsorption and critical-point wetting, has led to significant advances, both theoretical and experimental. It is probably not unjust to observe that the latter have been fewer and less striking than the former. Although observation and measurement have clearly demonstrated the existence of a variety of phenomena, theory, on the other hand, has demonstrated the sensitive dependence of the phenomena on the details of the intermolecular interactions. These developments are described in recent reviews [1–4]. In this article we report the findings of a pilot study using neutron reflectivity of wetting and adsorption in a pair of related binary liquid mixtures in the vicinity of their upper critical-solution point at an upper critical-solution temperature, T_{UCS}, and a critical mole fraction, x_c, or, more conveniently for some purposes, a critical volume fraction ϕ_c.

The phenomena of interest to us are the adsorption and wetting processes that occur at the so-called non-critical interface between the near-critical binary liquid mixture and, in the present case, an inert solid spectator phase. Although our measurements do not strictly correspond to the precise definition of a critical end-point, since the experimental vapour phase is air and not the coexisting vapour required for an end-point, our results refer to a system at a critical-solution point sufficiently close to a critical *end-point* to shed light on the principal features of the behaviour close to a true critical end-point. Accordingly,

‖ Present address: Department of Chemistry, University of Durham, Durham DH1 3LE, UK.

0953-8984/98/378173+16$19.50

henceforth we speak of critical points, and we believe that our conclusions can be taken as a good approximation to those that would emerge for a critical end-point. In principle, the spectator phase can be either the coexisting vapour or the inner wall of the solid container, but in this case it is the chemically modified polished plane face of a rectangular silicon block. The virtue of silicon for this purpose in our investigations is its near-transparency to neutrons of the wavelength available at the Institut Laue–Langevin where our measurements were made. Furthermore, well-known means exist to chemically engineer silicon surfaces so as to produce surfaces with varying but controlled and selective affinity for components of adjacent liquid systems.

Critical adsorption at a liquid-mixture interface [5] arises when the mixture of critical composition in its single phase $\alpha\beta$ approaches its critical-solution point whilst in contact with a non-critical (spectator) phase γ. Increasingly heavy adsorption of one of the mixture components occurs as the critical-solution point is approached, i.e. the surface excess or the relative adsorption of, say, component 2 with respect to component 1, $\Gamma_{2,1}$, goes to ∞ as $T \to T_{\mathrm{UCS}}$ for a mixture with $x = x_c$. Essentially, the interface thickness scales with the correlation length ξ of the composition fluctuations in the mixture.

Among the various forms of composition profile through the interface into the liquid phase which have been proposed, a common choice for representing the profile is the scaling form [6]

$$m(z) = m_0 t^{\beta} \left(\frac{\xi}{z} + c \right)^{\beta/\nu} \exp\left(-\frac{z}{\xi} \right) \tag{1}$$

where $m(z)$ is the order parameter normal to the interface (e.g. $m(z) = \phi(z) - \phi$, where ϕ is the bulk volume fraction and $\phi(z)$ is the volume fraction at distance z through the interface), $\beta = 0.325$ and $\nu = 0.63$ are critical exponents, m_0 is the bulk order-parameter amplitude, c is a tuning parameter, $t = |T - T_{\mathrm{UCS}}|/T_{\mathrm{UCS}}$, and ξ is the correlation length. The results of many ellipsometric measurements support the existence of profiles of such a form [7]. Critical adsorption also occurs when the liquid mixture has phase separated into coexisting liquid phases, here termed α and β. Although we do not here analyse our results using equation (1), neutron reflectivity in principle offers robust methods for studying the power-law behaviour inherent in this equation and its alternatives [8, 9].

Imagine, now, the point of contact between a solid container γ and the two liquid phases, α and β, of a phase-separated binary liquid mixture below an upper critical-solution point with $T < T_{\mathrm{UCS}}$. According to Cahn [10], at a wetting transition temperature T_{W}, usually in practice only a few degrees Kelvin from the critical temperature T_{UCS} of the mixture, one of the coexisting liquid phases β interposes itself between the solid wall γ and the other liquid phase α. In Cahn's work, this wetting transition is first order, although other authors found later that it could be a continuous transition (see Dietrich [3] for a review of the history). This difference in the order of the transition catalysed much theoretical work, and the solution was most elegantly presented by Dietrich and Schick [11]. At the centre of their theory is $\Omega_{\mathrm{S}}(l, T, \mu_i)$, the effective *interfacial* (i.e. per unit area) contribution to the grand canonical potential functional, given by

$$\Omega_{\mathrm{S}}(l, T, \mu_i) = l(\Omega_\beta - \Omega_\gamma) + \sigma_{\alpha,\beta} + \sigma_{\beta,\gamma} + \omega(l) \tag{2}$$

where l is the thickness of the layer of the interposed β-like phase at the α–γ interface, Ω_i is the grand canonical potential of *bulk* phase i (i.e. per unit volume), $\sigma_{i,j}$ is the interfacial tension between phases i and j, and $\omega(l)$ is the correction due to a finite thickness l of the wetting layer. Dietrich and Schick took into account long-range forces, and wrote $\omega(l)$ as

$$\omega(l) = a(T) l^{-2} + b(T) l^{-3} + \cdots \tag{3}$$

where the coefficients a and b (a is the Hamaker constant) can be written in terms of intermolecular potentials and densities. It is thus the temperature dependences of a and b, and their interplay, which determine the wetting behaviour of a given system. In particular, complete wetting, i.e. leading to the Antonow equality for the tensions at the line of contact, occurs if l_0, the wetting film thickness, equals infinity and $w(l)$ vanishes; a and b are thus the connection between theory and observation.

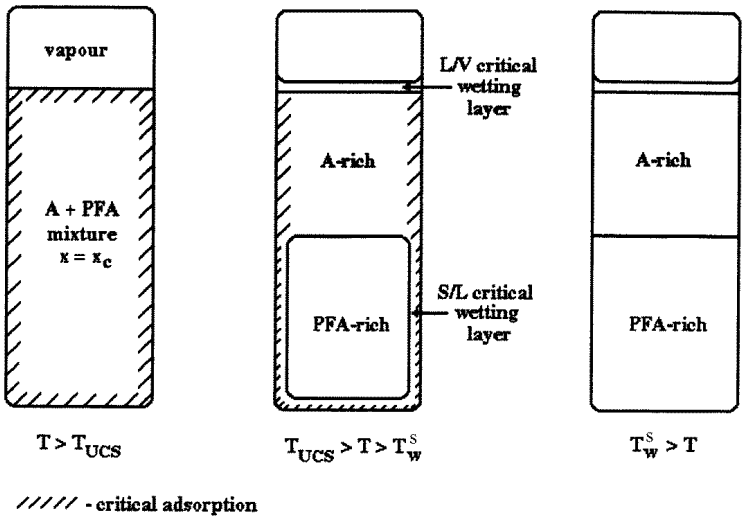

Figure 1. An outline of the adsorption and wetting characteristics for a typical alkane + perfluoroalkane mixture at the interfaces with the coexisting vapour and an alkane-like solid wall at three temperatures T: $T_W^v < T < T_W^s$; $T_W^s < T < T_{UCS}$; $T_{UCS} < T$, where T_W^s is the wetting transition temperature at the solid/liquid interface. At a still lower temperature there is a wetting transition at the liquid/vapour interface.

In practical terms, the relationship of critical adsorption and wetting is illustrated in figure 1. This shows the regions of critical-point adsorption and wetting for a class of mixture in which just inside the region of two-liquid-phase coexistence the upper phase wets the solid interface and much deeper into the two-phase region the lower phase wets the vapour interface. This pattern is that for the case of alkane + perfluoroalkane mixtures in contact with an alkane-like wall discussed in this paper. In the system under investigation we should expect the alkane to be critically adsorbed on an alkane-like wall, and this is what we observe. However, simple expectations as to the nature of the critically adsorbing component are not always borne out in practice, as Hirtz, Bonkhoff, and Findenegg have pointed out [12].

Experimentally, many approaches have been employed for investigating wetting transitions, most of which identify the existence of the transition—e.g. the capillary-rise experiments of Pohl and Goldberg [13]—but few of which offer much absolute structural detail about the thickness, composition or uniformity of the wetting layer. Ellipsometry is a useful structure-determining technique which has cast light on the order of the wetting transition via direct measurement of the layer thickness [14]. Evanescent-wave techniques are also useful for determining the compositions and thicknesses of adsorbed and wetting layers at the liquid-mixture/solid-wall interface [15–18].

However, in many cases the interpretation of experimental ellipsometry data relies upon certain tacit assumptions used in the theory of wetting transitions which, at least

at an experimental level, remain unverified. In the field of critical-point wetting, the main assumption applies to the uniformity and composition of the wetting layer. Often in the theory of wetting, a uniform slab of β-like phase is assumed to form the boundary layer, and with this assumption a layer thickness can be determined from the measured ellipticity. Thus far, this particular assumption has not been independently experimentally verified.

Specular neutron reflectivity has been applied extensively to the study of adsorption of surfactants and polymers at surfaces. It offers the capability of probing structure at solid/liquid and air/liquid interfaces without any technical limitations. Recently, it has been applied to the study of adsorption and wetting [8, 19]. Although a complete picture of the interface cannot be determined solely by neutron reflectivity, the technique offers some attractive, and at present almost unique, routes for exploring some aspects of adsorption profiles [9, 20]. Here we report the results of preliminary reflectivity experiments which probe the surface structure associated with adsorption and wetting at the solid/liquid interface, for a binary liquid mixture in the vicinity of its critical-solution point.

The liquid mixtures were *n*-hexane + perfluorohexane and *n*-heptane + perfluorohexane. These mixtures belong to the alkane + perfluoroalkane class of mixture that is characterized by liquid–liquid phase separation at temperatures not far below the normal boiling points of the components [21]. Since the components are available in a wide variety of chain lengths, particularly the alkanes, convenient upper critical-solution temperatures can readily be obtained by appropriate choice of chain lengths while scarcely affecting the generic behaviour.

Alkane + perfluoroalkane mixtures are eminently suitable for neutron reflectivity studies for two chief reasons. The first is that, since ^{19}F has a similar neutron scattering length to ^{2}H, similar advantages in contrast heightening attach to perfluoroalkane components as attach to the per- or polydeuterated species much used for contrast heightening in aqueous neutron reflectivity studies, notably of surfactant solutions. The second is that the intermolecular interactions are basically non-polar, so there is little known intrinsic structure in the liquid mixtures that might complicate the interpretation of the results. In relation to the present objectives listed below, we have selected alkane + perfluoroalkane mixtures which have been widely studied near their critical end-points, usually in the exact sense remarked on above, and so their near-critical behaviour is well established. In particular, the apparently weaker perfluoroalkane forces account for the initially surprising identification in most but not all alkane + perfluoroalkane mixtures of the perfluoroalkane-rich denser lower phase as the vapour-wetting component and the alkane-rich less-dense upper phase as the wall-wetting phase.

The phase diagram for *n*-hexane + perfluorohexane, shown in figure 2, illustrates that $T_{\mathrm{UCS}} = 22.61\ ^{\circ}\mathrm{C}$ at a bulk volume fraction ϕ very close to 0.5 corresponding to a mole fraction $x_c \sim 0.36$ [22, 23]. We have taken the volume fraction as $\phi = 0.5$, partly since this simplifies the calculation of the average scattering length densities Nb (see section 2.2), but partly also because we have employed this value for *n*-heptane + perfluorohexane without further enquiry since it has been shown that the liquid–liquid phase diagrams of alkane + perfluoroalkane mixtures are nearly all close to symmetrical in volume fraction, at least in the sense that $\phi_c \sim 0.5$ [24, 25]. The upper critical-solution temperature for *n*-heptane + perfluorohexane is higher than that for *n*-hexane + perfluorohexane with $T_{\mathrm{UCS}} = 43\ ^{\circ}\mathrm{C}$ [26].

A further advantage of alkane + perfluoroalkane mixtures in neutron reflectivity is that the option of resorting to perdeuterated alkane + perfluoroalkane mixtures is still fruitful and can be exploited to resolve problematic issues in undeuterated alkane + perfluoroalkane mixtures. This opportunity relies on the modest shift in thermodynamic behaviour

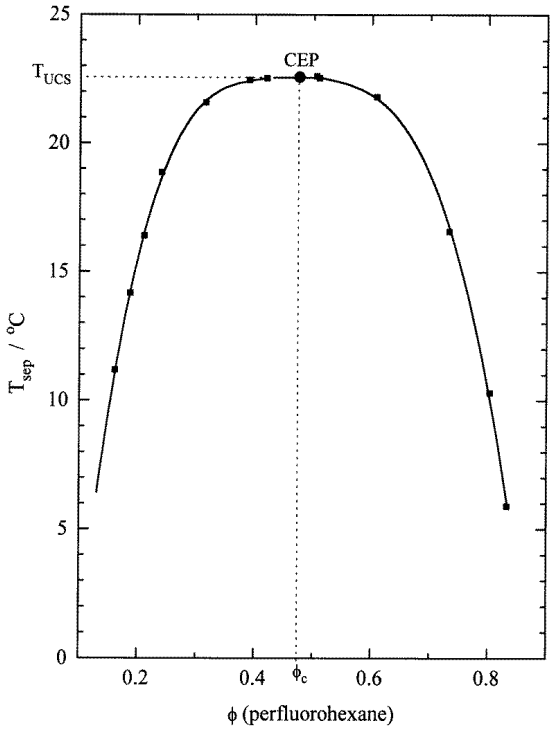

Figure 2. The liquid–liquid phase diagram for $(1-\phi)n$-hexane $+\,\phi$ perfluorohexane taken from references, where ϕ is the volume fraction [22, 23]. The critical point is marked ●. This diagram is qualitatively similar in form to that for $(1-\phi)n$-heptane $+\,\phi$ perfluorohexane.

occasioned by perdeuteration save for a shift of a few degrees Kelvin in critical temperature [27]. As we shall see, this is an opportunity which we shall find useful in future studies for resolving finer features of surface structure in the title mixtures near critical points.

Against this background, we have already explored the solid/liquid interface of the related mixture n-heptane + perfluorohexane near its T_{UCS} by evanescent-wave-generated-fluorescence spectroscopy [16, 17] and the liquid/vapour interface of n-hexane + perfluorohexane by neutron reflectivity [19, 28].

The anticipated sequence of wetting phenomena starting at high temperature is outlined in table 1 for a mixture in contact with an alkane-like wall, similar to the cases that we discuss in later sections. The sequence covers a range of temperatures embracing both the wetting transition temperature, T_W^s, at the solid/liquid interface and that, T_W^v, at the vapour/liquid interface, usually much further away from T_{UCS}.

Our principal general objective in this study was to assess the suitability of neutron reflectivity for studying critical adsorption and critical wetting in non-aqueous mixtures at solid surfaces, particularly as complementary to ellipsometry and evanescent-wave fluorescence spectroscopy. Our specific objectives were as follows.

(1) To determine the thickness of the adsorbed layer in the one-liquid-phase region at $T > T_{UCS}$.

(2) To confirm the identity and determine the thickness and uniformity of the wetting layer for $T < T_{UCS}$.

Table 1. The sequence of adsorption and wetting phenomena from above the critical-solution temperature T_{UCS} through the solid/liquid wetting transition temperature T_W^s to below the liquid/vapour transition temperature T_W^v.

	Upper phase		Lower phase
	Vapour/liquid interface	Solid/liquid interface	Solid/liquid interface
$T > T_{UCS}$	Perfluoroalkane critical adsorption	Alkane critical adsorption	N/A
$T_{UCS} > T > T_W^s$	Perfluoroalkane-rich wetting layer	Alkane adsorption	Alkane-rich wetting layer
$T_W^s > T > T_W^v$	Perfluoroalkane-rich wetting layer	Alkane adsorption	Modest alkane adsorption
$T_W > T$	Perfluoroalkane adsorption	Alkane adsorption	Modest alkane adsorption

2. Experimental procedure

2.1. Materials, sample preparation, equipment

The perfluorohexane, with nominal purity 99 mol% (of which 85% was the *n*-isomer), was purchased from Fluorochem, the *n*-heptane and *n*-hexane, of purity >99 mol%, were from Fluka, and the deuterium oxide, of 99 mol% purity, was from Fluorochem. All of the chemicals were used as received.

The sample cell used was similar in design to that used by Fragneto *et al* [29] but with minor changes essential for the specific requirements of our measurements. First, due to the volatility of the mixture components, a Viton O-ring was introduced into a recess in the polytetrafluoroethylene trough, and a seal was provided by pressing the silicon block ($80 \times 50 \times 15$ mm^3) against the O-ring. This produced a rectanguloid cavity for the liquid sample. Second, the trough was embedded in a cadmium-shielded copper block, ensuring good all-round thermal contact. The assembled cell temperature was controlled to within ± 0.1 °C by circulating ethylene glycol from a thermostat; the temperature was measured by a platinum resistance thermometer (Pt100) sited beneath the liquid in the underside of the polytetrafluoroethylene section.

The Si block was supplied, polished to ± 5 Å, by Holm Siliciumbearbeitung (Tann/Nieder Bayern, Germany). The silicon/silicon oxide SiO_2 surface was cleaned and activated according to the RCA standard procedure [30]. The block was first immersed in a cold 5:1:1-by-volume solution of Milli-Q water:hydrogen peroxide solution:ammonia solution (29%). The solution was then heated to 70–80 °C and maintained at that temperature for ten minutes; higher temperatures incur the risk of damage to the surface. The hot solution was then cooled by dilution with cold water. The last cleaning step involved successive immersion of the block in 1:1-by-volume and 1:3-by-volume methanol:trichloromethane mixtures and finally in pure trichloromethane. The coating on the block was formed during a two-hour immersion in the cold coating medium comprising a 70:20:10:1-by-volume decalin:tetrachloromethane:trichloromethane:octadecyltrichlorosilane (OTS) mixture. Finally, the block was rinsed in 0:1-by-volume, 1:1-by-volume, and 1:0-by-volume mixtures of methanol:trichloromethane.

Samples of the near-critical *n*-hexane + perfluorohexane mixture, with $x_c \sim 0.36$, were prepared by mass before transfer by syringe to the sample cell. Careful location of the filling holes leading to the sample cavity precluded the introduction of air bubbles. The

mixtures were *not* degassed. Despite care in mixture preparation, after phase separation the coexisting liquid-phase volumes were rather unequal. This made it difficult to selectively neutron illuminate one phase independently of the other phase. This manoeuvre lowers the neutron flux reflected from each phase and so incurs a detection statistics penalty. When it came to preparing the *n*-heptane+perfluorohexane solution, equal volumes of the coexisting phases at room temperature were used in order to study more directly the wetting behaviour in this system. The mixture was then of not exactly overall critical composition but this is essentially irrelevant for studies of coexisting liquid phases.

2.2. Measurements

The technique of neutron reflectivity has for the last decade been one of the most powerful methods for the determination of surface structure [31, 32], and has recently been applied successfully to the study of surfactant adsorption at silicon interfaces, chiefly from aqueous solution [29, 33]. In a neutron reflectivity experiment, the reflectivity R is measured as a function of Q, the momentum transfer normal to the reflecting surface:

$$Q = \frac{4\pi \sin\theta}{\lambda} \tag{4}$$

where λ is the neutron wavelength, and θ is the grazing angle of incidence of the neutron beam. The neutron refractive index can be approximated by

$$n \approx 1 - \frac{\lambda^2}{2\pi} Nb \tag{5}$$

where N is the number density of nuclei, and b the coherent scattering length of a nucleus. The multiple Nb is known as the scattering length density and is related in an approximately linear fashion to the volume fraction composition. The object of the analysis (inversion or model fitting) is then to associate the measured $R(Q)$ with a refractive index profile $n(z)$ or a scattering-length-density profile $Nb(z)$.

In order to remain close to the measurement observables, we have not converted the scattering length densities which emerge from the data analysis to compositions, so conforming to the seemingly accepted convention of employing scattering-length-density profiles $Nb(z)$ as effective measures of composition in the interfacial region. This is particularly reasonable with heterogeneous interfacial systems—like those discussed here—where adjacent layers usually need not contain contributions from all of the species of interest.

Reflectivities can be analysed by a number of techniques. These include the kinematic approximation where the data are inverted, layer models where the reflectivity is calculated using the Parratt formalism or the Abelès optical matrix method based on an assumed structural model, and model-independent methods [34, 35]. Our initial analysis was performed using a maximum-entropy method [36], but for simplicity the results presented here have been analysed using the optical matrix method assuming uncomplicated layer models. In the optical matrix method a layer model is constructed whereby each layer possesses a scattering length density Nb and a thickness d. Additionally, interlayer roughnesses σ can be introduced to help achieve the production of a smooth profile. The values of Nb for the materials used here are listed in table 2.

Neutron reflectivities were measured on the reflectometer D17 at the Institut Laue–Langevin, Grenoble, France. The beam axis is horizontal and the reflecting plane at the sample is vertical. This appealing characteristic was one of the reasons for choosing the D17 reflectometer for this experiment, since with this particular geometry and appropriate

Table 2. Scattering length densities Nb.

Material	$10^5 Nb/\text{Å}^{-2}$
Silicon	0.207
Deuterium oxide	0.638
Silicon oxide	0.360
Perfluorohexane	0.354
n-hexane	−0.04
n-heptane	−0.04
$C_{18}H_{37}$	−0.04

shielding we planned to investigate either of the upper or lower coexisting liquid phases in the same measurement run.

The incident neutron wavelength was 11 Å and the sample-to-detector distance was 2.88 m. The required Q-range of 0.005 to 0.25 Å^{-1} was obtained by altering the sample and detector angles in a standard θ–2θ geometry. The collimating slits were adjusted to maintain sample under-illumination; the slits were opened in proportion to the incidence angle, thus yielding reflectivities at constant relative angular resolution. The direct beam intensity as a function of the various slit openings was measured using a system of calibrated attenuators.

3. Results and discussion

3.1. Characterization of the silicon surface

In order to characterize the native silicon oxide layer and the layer of grafted $C_{18}H_{37}$ chains from the OTS which reside on the silicon surface, we performed three 'control' experiments. First, the reflectivity from the air/Si interface was measured (A). Second, the cell was assembled with the Si block in place and the reflectivity from the Si/air interface was measured (B), i.e. by bringing neutrons into the Si/air interface through the silicon rather than through air as in A, we thus cause B to be the inverse of A. If everything is in order with the cell, these two $R(Q)$ spectra should be satisfactorily modelled using the same set of surface parameters, i.e. we expect the interface structure to be the same. Finally, deuterium oxide was admitted to the cell and the reflectivity of the Si/D_2O interface was measured (C) with an eye to a subsequent investigation of the degree of penetration of the hydrophobic layer by the solution to compare with the work of Fragneto *et al* [29]. The resulting spectra were analysed using simple two-layer models; the Nb-profiles from the most consistent model together with the experimental and fitted reflectivities are shown in figure 3. In figure 3 and uniformly thereafter, $z = 0$ has been defined to fall at the Si/SiO_2 interface; note that in this case the subphase is the transmission medium and not the incidence medium. The scattering length densities, thicknesses of layers, and interlayer roughnesses are tabulated in table 3.

Fittings of the spectra measured in A and B reveal that the same parameters can be used; therefore there is no significant problem with the cell. However, at lower Q, approximately 0.015 Å^{-1}, there was a slight curvature of the spectrum absent in the results from A but apparent in those from B and C. We have not removed these data and the effect can be seen in figure 3(c) at low Q. We believe that this is the result of an edge effect caused by the cell/Si block edge where either the bevelled edge of the Si block or the Viton O-ring causes some obstruction. Test experiments were performed with different beam collimation

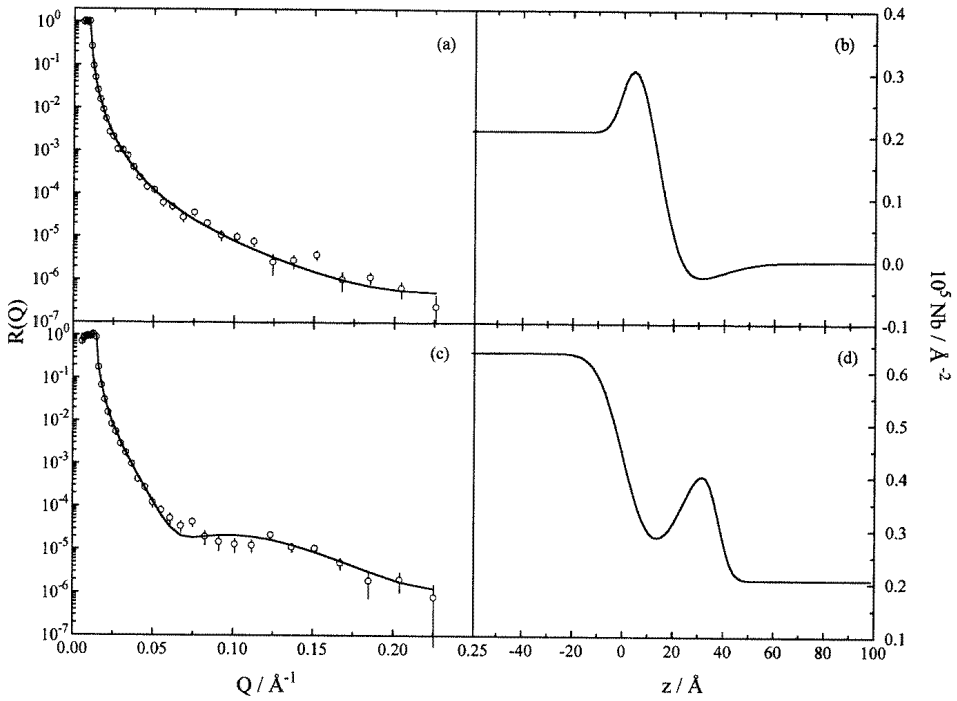

Figure 3. (a) Measured and modelled reflectivity spectra for the air/Si interface; (b) the scattering-length-density profile corresponding to the solid fit line in (a); (c) measured and modelled reflectivity spectra for the Si/D_2O interface; (d) the scattering-length-density profile corresponding to the solid fit line in (c).

Table 3. Fitting parameters for the calibration runs.

	Air			Deuterium oxide		
	d/Å	$10^5 Nb$/Å^{-2}	σ/Å	d/Å	$10^5 Nb$/Å^{-2}	σ/Å
Subphase		0			0.638	
			12			8
$C_{18}H_{37}$	24	−0.04		24	0.25	
			7			8
SiO_2	14	0.36		14	0.45	
			11			4
Si		0.207			0.207	

slit settings at small angles to see whether the effect could be removed by reducing the footprint (sample illumination) length. For all of the data points measured for $Q > Q'$, where Q' is some low-Q cut-off, the reflectivity was unaffected by the edge effect. In all of the spectra presented, the data points in this troublesome region have been retained.

In fitting the reflectivity from the deuterium oxide sample (C) we attempted to retain the parameters used to fit A and B as constant as possible. However, as reported by Fragneto *et al* [29], the hydrophobic layer is in fact not purely repulsive to water at a microscopic level. Some water can penetrate the grafted hydrophobic layer and the SiO_2 layer. Although

Fragneto *et al* report $\simeq$25% holes, in order to maintain consistency with A and B, we found it necessary to allow $\simeq$50% penetration. Due to this effect the value of Nb for the layers and the interlayer roughnesses may change slightly due to the actual adsorption profile. The thicknesses and values of Nb of both the SiO_2 and the $C_{18}H_{37}$ layers agree with those of Fragneto *et al*. Whilst these authors characterized their surface-layer parameters assuming zero interlayer roughness, the need for constancy of the surface parameters (even permitting solvent ingress in the surface layers) prevents us from ignoring the roughness for the spectra that we measured. In reality, this may be the source of the inconsistency in the penetration quantities listed.

In the present case we wished to compare our characterization results with those of Fragneto *et al*, but in future measurements we shall use *n*-hexane or d_{14}-*n*-hexane for the secondary calibration (C) to avoid adding unnecessary impurities into the cell.

Following the calibration runs, the cell was rinsed with ethanol and copious quantities of *n*-hexane before admitting a single-phase sample of *n*-hexane + perfluorohexane.

3.2. The fitting strategy

Due to non-uniqueness problems in the fitting of reflectivity spectra, we have adopted a fitting with the minimum number of layers, and hence fitting parameters, which can describe the data adequately—so applying a 'minimum information' or *Ockham's razor* condition. First of all, we assumed that the surface is constituted from, at most, three layers: the SiO_2, the $C_{18}H_{37}$ layer, and an adsorbed layer with undefined Nb, d, and σ. The latter parameters for these layers are determined from fitting the $R(Q)$ profiles. Occasionally, when modelling the adsorption region with a single layer, highly unphysical roughnesses emerged, so indicating that the single-layer model was oversimplified. However, introducing no more than one additional layer gave in all cases a satisfactory description of $R(Q)$ without unrealistic features in the scattering-length-density profile. Initially, of course, we neglect the inclusion of the adsorbed layer to see whether a model without adsorption is sufficient. Furthermore, in addition to an adsorbed layer, we also permit the intrusion of the mixture into the surface layers. As a result of the solution-space ambiguity, we cannot determine the exact amount of fluid penetration, but fortunately there is sufficient flexibility in the fitting parameters to account for the resulting uncertainties without significantly altering the salient features of the underlying model. Some of the spectra are noisy, resulting from the necessity to mask off one of the liquid phases. Owing to the time limitations of the experiment, we were unable to collect for the requisite long time periods. Despite this limitation, the effect of the noise is largely cosmetic, and does not dramatically affect the outcome of the analysis. To account for these factors, we present simple models which contain the essential information that we are seeking, describe the data adequately, and do not contradict other findings.

We now turn to the results for mixtures. Although we made many measurements at different temperatures down to around 0 °C, we report here only results at a few selected representative temperatures which illustrate the characteristic features of the resulting profiles. In all of the scattering-length-density profiles, $Nb(z)$, shown, we define $z = 0$ at the feature, sharp on the scale of wetting-layer thicknesses, corresponding to the invariant Si/SiO_2 boundary.

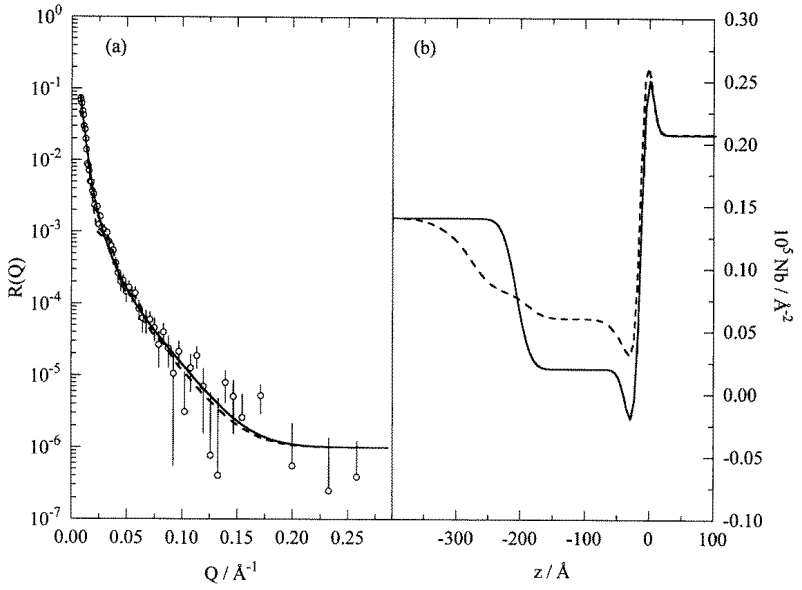

Figure 4. (a) Measured and modelled reflectivity spectra for the Si/liquid interface where the liquid is a critical mixture with $x_c = 0.36$ of *n*-hexane + perfluorohexane ($10^5 Nb = 0.14$ Å^{-2}) in its single liquid phase at 27.9 °C ($T_{\mathrm{UCS}} = 22.61$ °C). (b) Scattering-length-density profiles with the solid and dashed lines corresponding to the solid and dashed fit lines in (a).

3.3. n-hexane + perfluorohexane in the one-phase region

Reflectivity spectra were measured from a sample with $x \sim x_c = 0.36$ at several temperatures in the range $23 < T/^{\circ}\mathrm{C} < 28$, i.e. just above $T_{\mathrm{UCS}} = 22.6$ °C. The reflectivity does not change significantly beyond the experimental error with T as T approaches T_{UCS}. from above. Consider as typical the measurements made at $T = 27.9$ °C as displayed in figure 4(a); the collection statistics are reasonably good and are representative of those for spectra at other temperatures in this region. Some rather ill-resolved fringes—indicative of the presence of a thick layer—are apparent in the spectrum, and models could be generated which reproduced them to some extent. In figure 4 the measured and calculated reflectivities for such models and the corresponding Nb-profiles are shown.

In both fits, as in the case of the deuterium oxide, there were signs of some degree of penetration by the mixture—or at least by some *n*-hexane-rich liquid—into the surface layers. The extent of penetration is uncertain and slightly different for the two fits. In each case the surface is enriched by a thick—$\simeq$250 Å—*n*-hexane-rich layer. The major difference between the models is the greater diffuseness of the model with the less-hexane-rich layer near the $C_{18}H_{37}$-layer/bulk-mixture interface. We have no ready explanation for the observation of this 250 Å *n*-hexane-rich layer, and so defer comment until we are able to investigate in greater detail the conditions for its occurrence. Simulation suggests that the profile on the liquid side is not well represented by an exponential decay.

Future experiments, with better collection statistics and using perdeuterated rather than undeuterated *n*-hexane, to attain total reflection more easily, will attempt to verify or discount the form of the Nb-profile. These measures will sharpen the appearance of the interference fringes just perceptible in our present measurements but insufficiently resolvable to yield

unambiguous diagnostic information. We should not expect critical adsorption in this region, because except very close to T_{UCS} we find ξ very close to ξ_0.

3.4. n-hexane + perfluorohexane in the two-phase region

The temperature of the reflectivity cell could not be reduced sufficiently to observe the solid/liquid wetting transition in this system, and chiefly for that reason we turned to *n*-heptane + perfluorohexane which has a higher value of T_{UCS} at 46 °C [26], and a correspondingly more accessible solid/liquid wetting transition temperature. However, the results for the *n*-hexane-containing mixture are reasonably straightforward to report, and we do so for completeness, for comparison with the *n*-heptane + perfluorohexane results in the next section. The reflectivity spectra shown in figure 5 were measured for the upper and lower phases at $T = 11.6$ °C. The upper *n*-hexane-rich phase can be modelled simply by allowing some mixture to penetrate both the $C_{18}H_{37}$ layer—which does not alter its value of Nb significantly—and the SiO_2 layer—which does lower its value of Nb slightly. Apart from the slight variations in Nb, the fitted layer thicknesses remain unchanged. Arguably, there are some fringes in the lower spectrum in figure 5(a) which have not been taken into account in the calculated reflectivity. However, the data are too noisy to sustain a more detailed analysis, and, besides, the simple model does describe the salient features of $R(Q)$.

The spectrum for the lower phase (the uppermost spectrum in figure 5(a)) is slightly more difficult to model since it is particularly noisy. The two reflectivity spectra shown in figure 5(a) are extremely alike. The spectrum of the lower phase can be described by either of two models, but indistinguishably with the experimental information available at

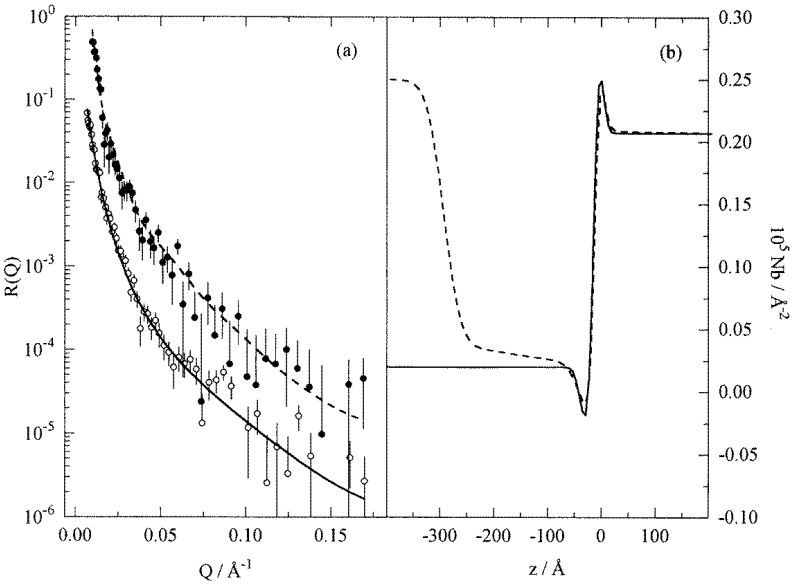

Figure 5. (a) Measured and modelled reflectivity spectra for the Si/liquid interface where the liquid is a mixture with $x_c = 0.36$ of *n*-hexane + perfluorohexane in two phases at 11.6 °C ($T_{UCS} = 22.61$ °C). The upper spectrum is for the Si/lower-phase interface (and is shifted upwards by one order of magnitude) and the lower spectrum is for the silicon/upper-phase interface. (b) Scattering-length-density profiles with the solid and dashed lines corresponding to the solid (upper-phase) and dashed (lower-phase) fit lines in (a).

present. Further measurements are necessary to resolve matters. The first model consists of a macroscopically thick wetting layer of the *n*-hexane-rich phase at the interface. In the second model, by assuming that the underlying subphase is a perfluorohexane-rich phase with $10^5 Nb = 0.25$ Å^{-2} (from the phase diagram [22, 23] without excess-volume correction), then a wetting layer with thickness $\simeq$300 Å can be proposed, which is consistent with predicted and reported values of wetting layers in the literature (e.g. see [3]).

The multidetector or off-specular results indicate the presence of a Yoneda peak at very low Q, consistent with an (unobserved) very small critical edge. This observation slightly favours the model incorporating a layer 300 Å thick over that with the macroscopic hexane-rich layer. It stands in contrast to the heptane + perfluorohexane results discussed below, in which there is also a Yoneda peak but in this case vanishing at high temperatures, implying a transition from a thin wetting layer to a macroscopic layer.

The Nb-profiles which permit adequate fitting of the measured reflectivities are shown in figure 5(b). In contrast to the modelled adsorption above T_{UCS}, the wetting layer is reasonably sharply defined. The main point of note is that the composition of the wetting layer, within the model fitting used here, is not of a constant composition throughout. Once again, as with the observation for the thick *n*-hexane-rich layer, we have no ready explanation to account for this highly unexpected interfacial feature; we hope to make measurements later which will focus on this part of the interface.

After withdrawing the liquid from the sample cell, it was noted that the volumes of the two phases were not equivalent; therefore the measured spectra could be 'contaminated' with an unwanted signal from the other phase, despite the shielding measures taken. Furthermore, reduction of the temperature did not induce a detectable dewetting transition. This latter point may be due to the lack of stirring available in the cell and the slow dissipation of the wetting film. We now turn to a similar system in order to see whether wetting does occur on raising the temperature.

3.5. n-heptane + perfluorohexane in the two-phase region

Recently we have used evanescent-wave-generated-fluorescence spectroscopy to study the wetting transition for the *n*-heptane + perfluorohexane mixture in contact with a quartz surface [18]. Here, we sought information on a wetting transition for the same mixture but with a somewhat different substrate. Although many authors report that $T_{\mathrm{W}}^{\mathrm{s}}$ for solid/liquid interfaces lies $\simeq$10 K from T_{UCS}, our measurements on *n*-hexane+perfluorohexane suggested that $|T_{\mathrm{UCS}} - T_{\mathrm{W}}^{\mathrm{s}}|$ is rather greater and thus inaccessible in the experimental arrangement in use. We therefore turned to *n*-heptane + perfluorohexane in order to make measurements at temperatures with larger values of $|T_{\mathrm{UCS}} - T_{\mathrm{W}}^{\mathrm{s}}|$.

After the cell had been rinsed with *n*-heptane, the sample cell was loaded with two equi-volume phases and the reflectivities from the upper and lower phases were measured at two temperatures, 4.8 °C and 39.5 °C. As expected with the $C_{18}H_{37}$ surface coating, the *n*-heptane-rich phase wets the Si/perfluorohexane-rich phase interface. At $T = 4.8$ °C, the spectra can be fitted, and the fits and the so-determined Nb-profiles are shown in figure 6. The spectra measured from the Si/SiO_2/coexisting phase interfaces at the lower temperature are distinctly different—see figure 6(a)—and this difference cannot be accounted for with respect to the low-Q problems mentioned in section 3.1. Once again the model used to fit the upper-phase reflectivity is, as expected, unsurprising—the Nb-profile is shown in figure 6(b). At the lower phase boundary, there is a $\simeq$200 Å *n*-heptane-rich wetting layer at the interface.

At $T = 39.5$ °C, however, the upper- and lower-phase $R(Q)$ spectra are not significantly

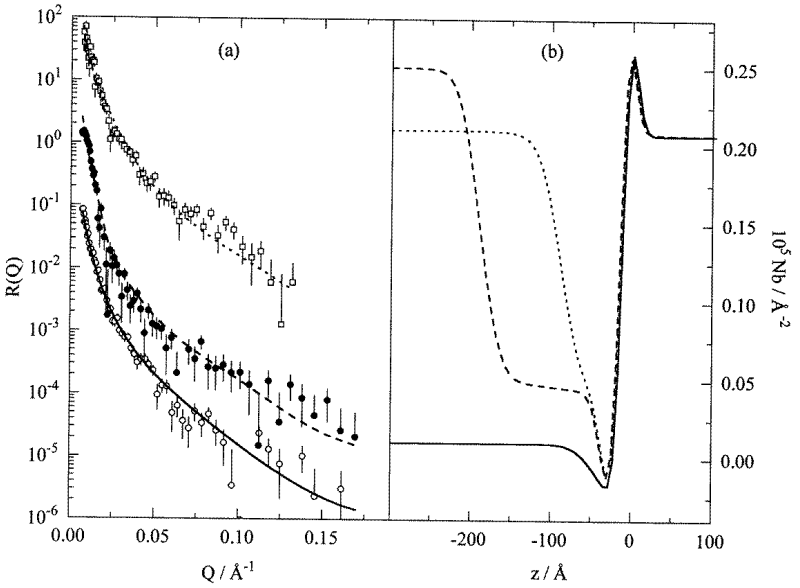

Figure 6. (a) Measured and modelled reflectivity spectra for the Si/liquid interface where the liquid is an equi-phase volume mixture of *n*-heptane + perfluorohexane in two phases (T_{UCS} = 43 °C). The upper spectrum is for the Si/lower-phase interface at 39.5 °C (shifted up by three orders of magnitude), the middle spectrum is for the Si/lower-phase interface at 4.8 °C (shifted up by one order of magnitude), and the lower spectrum is for the Si/upper-phase interface at 4.8 °C. (b) Scattering-length-density profiles with the solid, dashed and dotted lines corresponding to the solid (the upper phase at 4.8 °C), dashed (the lower phase at 4.8 °C), and dotted (the lower phase at 39.5 °C) fit lines in (a).

different. There is a uniqueness problem in determining the structure. Either the thickness of the *n*-heptane-rich wetting layer at the Si/lower-phase boundary becomes macroscopic, or otherwise the layer thins from ≃200 Å to ≃50 Å, signifying an unlikely thinning of the layer.

However, the multidetector spectrum supports the former of these two models, i.e. the macroscopic wetting model. At $T = 4.8$ °C the multidetector spectrum for the lower phase displays a distinct Yoneda peak—the signature of total external reflection—which vanishes at $T = 39.5$ °C, suggesting the formation of a macroscopically thick phase which does not permit total reflection from the Si/liquid interface. Certainly, the introduction of d_{14}-*n*-hexane would aid interpretation of this result and would also provide a more direct measure of the composition of the wetting layer.

4. Conclusions

The results of the measurements reported here demonstrate that neutron reflectivity is indeed a suitable technique for the study of adsorption and wetting in near-critical non-surfactant systems at solid/liquid interfaces. This was our principal objective in undertaking this investigation.

Despite the limitations upon the interpretation of the data, the presence of wetting layers has been demonstrated along with hitherto unavailable direct evidence of the composition profile of the layer. From fitting the spectra using simple layer models, the resulting models

give information about the form of the bulk-liquid/wetting-layer interface, the composition and uniformity of the wetting layer, and the penetration of the hydrophobic layer by the components of the mixture. In particular, in respect of the specific objectives set out in the introduction, we can list the following conclusions.

(1) We have found that the thickness of the region of hexane-rich adsorption in *n*-hexane + perfluorohexane in the one-liquid-phase region 5 K above T_{UCS} is about 250 Å, despite some ambiguity in the two models employed. With the information thus far available, it is unclear how these profiles evolve with temperature, since the measured spectra did not alter significantly at other temperatures for $T > T_c$. This is clearly an objective for future work with isotopic substitution.

(2) In the $T < T_{UCS}$ region, the wetting layer is either about 300 Å thick—and favoured by the presence of a Yoneda peak—or macroscopic, for *n*-hexane + perfluorohexane about 12 K below T_{UCS}. For *n*-heptane + perfluorohexane, the layer thickness is about 200 Å at 4.8 °C, some 38 K below T_{UCS}, and macroscopic at 39.5 °C, about 3.5 K below T_{UCS}. The scattering length density in the wetting layers in all cases is similar to that in the bulk wetting phase determined from the experimental phase diagram.

The non-uniqueness problem, which is well represented, especially in section 3.5, highlights the need to use other, complementary, techniques to determine different facets of wetting phenomena. Nevertheless, neutron reflectivity measurements offer unique information on non-critical interfaces near critical-solution points. Accordingly, further, more detailed measurements both on these and on related mixtures are planned. They will incorporate isotope substitution and better measuring statistics, and, with the improvements to reflectometer D17 currently in progress, they should provide more comprehensive and more dependable information about the nature of wetting layers than we have reported here.

Acknowledgments

The authors thank the workshop of the Iwan Stranski Institute for the careful construction of the experimental cell, and the ILL for provision of beamtime on the reflectometer D17. JB thanks the European Commission for grant number ERBFMBICT961176 on the TMR programme, and Professor G H Findenegg for accommodation in his laboratory during this project. EMP acknowledges with thanks the provision of a scholarship from CONACyT, Mexico.

References

[1] Blokhuis E M and Widom B 1996 *Curr. Opin. Colloid Interface Sci.* **1** 424
[2] Findenegg G H and Herminghaus S 1997 *Curr. Opin. Colloid Interface Sci.* **2** 301
[3] Dietrich S 1988 *Phase Transitions and Critical Phenomena* vol 12, ed C Domb and J L Lebowitz (London: Academic)
[4] Schick M 1990 *Liquides aux Interfaces* ed J Charlovin, J F Joanny and J Zinn-Justin (Amsterdam: North-Holland)
[5] Fisher M E and de Gennes P G 1978 *C. R. Acad. Sci., Paris* **287** 207
[6] Liu A and Fisher M E 1989 *Phys. Rev.* A **40** 7202
[7] Smith D S P, Law B M, Smock M and Landau D P 1995 *Phys. Rev.* E **55** 620
[8] Zhao H, Pennickx-Sans A, Lee L-T, Beysens D and Jannink G 1995 *Phys. Rev. Lett.* **75** 1977
[9] Dietrich S and Schick R 1987 *Phys. Rev. Lett.* **58** 140
[10] Cahn J W 1977 *J. Chem. Phys.* **66** 3667
[11] Dietrich S and Schick M 1986 *Phys. Rev.* B **33** 4952
[12] Hirtz A, Bonkhoff K and Findenegg G H 1993 *Adv. Colloid Interface Sci.* **44** 241

[13] Pohl D W and Goldburg W I 1982 *Phys. Rev. Lett.* **48** 1111
[14] Bonn D, Kellay H and Wegdam G H 1994 *J. Phys.: Condens. Matter* **6** A389
[15] Beysens D and Leibler S 1982 *J. Physique Lett.* **43** L133
[16] Bowers J, Clements P J and McLure I A 1996 *Physica* A **234** 239
[17] Williamson A-M and McLure I A 1996 *Physica* A **234** 225
[18] McLure I A and Williamson A-M 1996 *Physica* A **234** 206
[19] Bowers J, Clements P J, Burgess A N and McLure I A 1996 *Mol. Phys.* **89** 1825
[20] Sans A and Jannink G 1994 *Ber. Bunsenges. Phys. Chem.* **98** 481
[21] Swinton F L 1978 Mixtures containing a fluorocarbon *Chemical Thermodynamics* vol 2, ed M L McGlashan (London: The Chemical Society) ch 5, pp 147–73
[22] Clements P J, Zafar S, Galindo A, Jackson G and McLure I A 1996 *J. Chem. Soc. Faraday Trans.* **93** 1331
[23] Bedford R G and Dunlap R D 1958 *J. Am. Chem. Soc.* **80** 282
[24] Gilmour J B, Zwicker J O, Katz J and Scott R L 1967 *J. Phys. Chem.* **71** 3259
[25] Munson M S B 1964 *J. Phys. Chem.* **68** 796
[26] Archer A L, Amos M D, Jackson G and McLure I A 1996 *Int. J. Thermophys.* **17** 201
[27] Batchelor H, Clements P J and McLure I A 1996 *J. Chem. Soc. Faraday Trans.* **92** 2255
[28] Bowers J, Whitfield R, Burgess A N, Eaglesham A and McLure I A 1997 *Langmuir* **13** 2167
[29] Fragneto G, Lu J R, MacDermott D C, Thomas R K, Rennie A R, Gallacher P D and Satija S K 1996 *Langmuir* **12** 477
[30] Kern W 1990 *J. Electrochem. Soc.* **137** 1887
[31] Penfold J and Thomas R K 1990 *J. Phys.: Condens. Matter* **2** 1369
[32] Penfold J, Richardson R M, Zarbakhsh A, Webster J R P, Bucknall D G, Rennie A R, Jones R A, Cosgrove T, Thomas R K, Higgins J S, Fletcher P D I, Dickinson E, Roser S J, McLure I A, Hillman A R, Richards R W, Burgess A N, Simister E A and White J W 1997 *J. Chem. Soc. Faraday Trans.* **93** 3899
[33] Thirtle P N, Li Z X, Thomas R K, Rennie A R, Satija S K and Sung L P 1997 *Langmuir* **13** 5451
[34] Kunz K, Reiter J, Götzelmann A and Stamm M 1993 *Macromolecules* **26** 4316
[35] Zhou X-L and Chen S-H 1993 *Phys. Rev.* E **47** 3174
[36] Sivia D S, Hamilton W A and Smith G S 1993 *Physica* **173** 121